Open Access Full Text Article

ORIGINAL RESEARCH

Cerium oxide nanoparticles promote neurogenesis and abrogate hypoxia-induced memory impairment through AMPK–PKC–CBP signaling cascade

Aditya Arya[1]
Anamika Gangwar[1]
Sushil Kumar Singh[2]
Manas Roy[3,4]
Mainak Das[3]
Niroj Kumar Sethy[1]
Kalpana Bhargava[1]

[1]Peptide and Proteomics Division, Defense Institute of Physiology and Allied Sciences, [2]Functional Materials Division, Solid State Physics Laboratory, Defense Research and Development Organization, Timarpur, Delhi, [3]Biological Science and Bioengineering, Indian Institute of Technology, Kanpur, [4]Department of Chemistry, Indian Institute of Engineering Science and Technology, Howrah, India

Correspondence: Kalpana Bhargava;
Niroj Kumar Sethy
Peptide and Proteomics Division, Defense Institute of Physiology and Allied Sciences, Defense Research and Development Organization, Lucknow Road, Timarpur, Delhi 110054, India
Tel +91 11 2388 3010; +91 11 2388 3003
Fax +91 11 2393 2869; +91 11 2393 2869
Email kalpanab2006@gmail.com; nksethy@gmail.com

Abstract: Structural and functional integrity of the brain is adversely affected by reduced oxygen saturation, especially during chronic hypoxia exposure and often encountered by altitude travelers or dwellers. Hypoxia-induced generation of reactive nitrogen and oxygen species reportedly affects the cortex and hippocampus regions of the brain, promoting memory impairment and cognitive dysfunction. Cerium oxide nanoparticles (CNPs), also known as nanoceria, switch between +3 and +4 oxidation states and reportedly scavenge superoxide anions, hydrogen peroxide, and peroxynitrite in vivo. In the present study, we evaluated the neuroprotective as well as the cognition-enhancing activities of nanoceria during hypobaric hypoxia. Using polyethylene glycol-coated 3 nm nanoceria (PEG-CNPs), we have demonstrated efficient localization of PEG-CNPs in rodent brain. This resulted in significant reduction of oxidative stress and associated damage during hypoxia exposure. Morris water maze-based memory function tests revealed that PEG-CNPs ameliorated hypoxia-induced memory impairment. Using microscopic, flow cytometric, and histological studies, we also provide evidences that PEG-CNPs augmented hippocampus neuronal survival and promoted neurogenesis. Molecular studies revealed that PEG-CNPs promoted neurogenesis through the 5′-adenine monophosphate-activated protein kinase–protein kinase C–cyclic adenosine monophosphate response element-binding protein binding (AMPK-PKC-CBP) protein pathway. Our present study results suggest that nanoceria can be translated as promising therapeutic molecules for neurodegenerative diseases.

Keywords: cerium oxide nanoparticles, oxidative stress, memory, hypoxia, neuroprotection

Introduction

The partial pressure of oxygen in the inspired air diminishes with the increase in altitude, resulting in hypobaric hypoxia and compromised supply of oxygen to the tissues. Brain is the first organ to be compromised in response to low oxygen levels.[1,2] Moreover, inadequacy of cerebral oxygen delivery systems during chronic hypobaric hypoxia results in adverse consequences such as neuroinflammation, high-altitude cerebral edema, motor impairment, memory impairment, and cognitive dysfunctions, along with structural alterations of brain.[2–5] Hypoxia induces the cells to undergo anaerobic glycolysis, as well as shifts the glucose metabolism from mitochondria to glycolysis, which partially compensates the cellular energy demand.[6,7] Concomitantly, hypoxia also causes oxidative stress from uncontrolled generation of mitochondrial reactive oxygen species (ROS) that may be detrimental for cell survival.[7–9] We, along with others, have previously reported that brain regions such as hippocampus and cortex are more vulnerable to hypoxic oxidative damage.[8,10,11] This hypoxia-induced pronounced oxidative stress also promotes neurodegeneration and spatial memory impairment.[8,12]

Hippocampus is the key site for long-term memory formation and viability of hippocampal neurons and is therefore obligatory for cognition.[13–16] Unfortunately, a deficient antioxidant defense system, higher content of polyunsaturated fatty acids, along with abundance of transition metals such as iron and copper facilitating Fenton's reaction make the hippocampus vulnerable to hypoxia-induced oxidative damage and adversely affect cognition.[8–11] Studying the effect of hypobaric hypoxia on memory impairment, Maiti et al[8,12] have reported that hypoxia-induced oxidative stress and neuronal apoptosis in brain regions such as hippocampus, cortex, and striatum significantly affect spatial reference memory. With respect to hippocampus, it has been reported that the CA3 neurons are more susceptible to hypoxia-induced cell death than CA1 neurons. These studies suggest the deleterious roles of hypoxia-induced oxidative stress in promoting alterations to hippocampal neuronal morphology, neuronal degeneration, apoptosis, and cognitive dysfunction. It has been suggested that timely intervention of antioxidants may curtail oxidative damage during hypoxia.[9]

Cerium oxide nanoparticles (CNPs) possess excellent catalytic activities (both oxidation and reduction catalyst), which are derived from transition of oxidation states between Ce^{3+} and Ce^{4+}.[17–19] They also exhibit oxygen vacancies in the lattice structure that augment their antioxidant capacity.[20] Moreover, CNPs reportedly possess enzyme mimetic properties of superoxide dismutase, catalase, peroxidase, oxidase, as well as scavenge hydroxyl and nitric oxide radicals.[20,21] The in situ regeneration of antioxidant properties depending on the biological environment is highly desirable[22] and repeated supplementation is not required unlike conventional antioxidants. Because of these properties, nanoceria have been extensively studied for their antioxidant properties in several biological systems. The neuroprotective efficacies of nanoceria have been studied in adult rat spinal cord neurons,[23] brain slice model of ischemia,[24] animal models of ischemic stroke,[25] multiple sclerosis,[26] and Parkinson's disease.[27] These studies have reported efficient neuroprotection activities of nanoceria, primarily by reducing nitrosative stress.[24,27,28]

In this study, we evaluated the neuroprotective efficacy as well as cognition-promoting activities of CNP nanoparticles during chronic hypobaric hypoxia. Using polyethylene glycol (PEG) coating, we ensured brain delivery and penetration of CNPs within the brain tissue,[25,29–31] which was confirmed by imaging studies. Brain-localized PEG-CNPs minimized hypoxia-induced oxidative stress and neuronal apoptosis. Interestingly, PEG-CNPs also ameliorated hypoxia-induced memory impairment and promoted hippocampal neurogenesis. We further investigated neurogenesis activities of nanoceria using an array of techniques, including microscopy, flow cytometry, and histology. Our studies reveal that nanoceria promote neurogenesis via 5′-adenine monophosphate-activated protein kinase (AMPK)-mediated phosphorylation of protein kinase C (PKCζ) and activating cyclic adenosine monophosphate response element-binding protein (CREB) binding protein (CBP). These results suggest the therapeutic potential of PEG-CNPs for improving cognition in a variety of neurogenerative disorders.

Materials and methods
Materials
All the chemicals and reagents were purchased from Sigma-Aldrich (St Louis, MO, USA) unless specified otherwise in the following section.

Experimental design and ethics statement
All the animal care and experimental protocols were approved by Defense Institute of Physiology and Allied Sciences animal ethical committee under the supervision of Committee for the Purpose of Control and Supervision of Experiments on Animals (CPCSEA), Ministry of Environment and Forest, Government of India.

Adult male Sprague Dawley rats of age 6 weeks were used in the study. All the animals were housed at controlled temperature (25°C±2°C) and humidity (65%±5%) in 12/12 hour day and night cycle with food and water available ad libitum. Forty-eight rats were randomly divided into two groups (n=24) as control and PEG-CNPs supplemented. Five micrograms of PEG-CNPs in 100 μL in phosphate-buffered saline (PBS) (50 μg/mL) were administered to animals via intraperitoneal route in three successive doses on a weekly basis. During the route optimization, intravenous (IV) and peroral routes were also chosen for administration of the drug. Both the experimental groups were subjected to Morris water maze (MWM) behavioral assay for 8 days, and then 12 animals from the control group and 12 animals from PEG-CNPs group were exposed to hypobaric hypoxia for 10 days and were named hypoxia and PEG-CNPs + hypoxia groups, respectively. Both groups were again subjected to MWM test. Remaining animals were euthanized and their brains were isolated and stored under liquid nitrogen till further experimentation. Finally, the animals from hypoxia and PEG-CNPs + hypoxia groups were also euthanized and their plasma and brain tissues were harvested and used immediately for further experimentation. Figure 1 illustrates the experimental design.
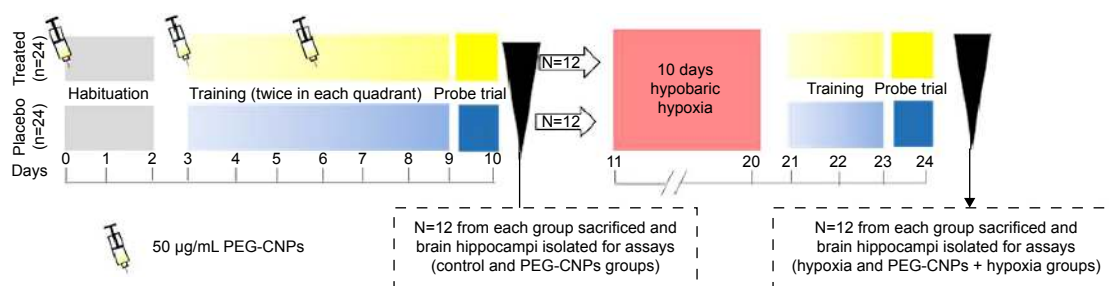
Figure 1 Schematic of experimental design.
Notes: The animals were randomly divided into two groups (n=24 each); one group received PEG-CNPs injection (concentration 5 μg/kg BW, intraperitoneally) and the other group received normal saline (phosphate-buffered saline). Animals were habituated for 2 days by keeping them in the room containing MWM and placing them in water for 5 minutes each day. Next the animals were randomly divided into two groups. The second dose (out of the three) was administered on third day before beginning the Morris Water Maze experiments. Third dose of PEG-CNPs was injected on the sixth day, and after 7 days of training, in each quadrant, 12 animals from each group were subjected to probe trial, while the remaining 12 animals were exposed to hypobaric hypoxia (10 days). These groups were renamed as hypoxia (without PEG-CNPs injection) and hypoxia + PEG-CNPs groups. After 10 days of hypoxia, animals were again subjected to MWM learning for 2 days followed by probe trial.
Abbreviations: CNPs, cerium oxide nanoparticles; MWM, Morris water maze; PEG, polyethylene glycol.

Hypobaric hypoxia exposure

Hypoxia and PEG-CNPs + hypoxia animals were subjected to simulated hypobaric hypoxia for 10 days. The animals were exposed to a simulated altitude of 25,000 ft (7,620 m, 282 mmHg) in a specially designed hypobaric chamber in which the altitude could be maintained by reducing the barometric pressure by air suction pumps. The exposure was continuous for 10 days except for a 15-minute interval after each 48 hours for the replacement of cage, water, and food. Fresh air was continuously flushed into the chamber at a constant rate of 8 L/min. The chamber temperature was maintained at 25°C±2°C, and humidity was kept 65%±5%. Also, a 12–12 hour day night cycle was maintained for animal housing.

Synthesis and characterization of PEGylated CNPs

PEGylated CNPs (PEG-CNPs) were synthesized by aqueous route using cerium (III) nitrate hexahydrate [$Ce(NO_3)_2 \cdot 6H_2O$], polyethylene glycol-8000 (PEG-8000) (Sigma-Aldrich), ceric ammonium nitrate [$(NH_4)_2Ce(NO_3)_6$] (Nice Chemicals, Gurgaon, India), and ammonia solution (Rankem, Center Valley, PA, USA). In brief, an equimolar mixture (0.01 M each) of $Ce(NO_3)_2 \cdot 6H_2O$ and $(NH_4)_2Ce(NO_3)_6$ was added to 1% w/v aqueous solution of PEG-8000 in drop wise manner with continuous stirring to reach a final concentration of 0.5 μM. Further, after complete solubilization, 2.5 mL of 1 M NH_4OH was gradually added to this mixture. Once an off-white colloid suspension started to form (~0.5 hours), the solution was constantly stirred for 4 hours to allow complete hydrolysis of the salts. The colloidal was then incubated at room temperature for 1 hour to complete the nucleation process. Finally, the solution was centrifuged at approximately $7,500\times g$ for 3 minutes. The precipitate was washed thrice with ion-free water to remove water-soluble impurities and three times with acetone. The obtained precipitate was desiccated and vacuum dried for further use. The particle size and morphology were determined using phase-contrast high-resolution transmission electron microscope (TEM; Philips Technai G230 TEM, OR, USA) operating at an accelerating voltage of 300 kV and equipped with energy-dispersive spectrometry and selected area electron diffraction (SAED). X-ray diffraction (XRD) patterns were measured with a Bruker D8 Advance and a Rigaku miniflex-(II) X-ray (Billerica, MA, USA) diffractometer employing monochromatized Cu Kα radiation (α=1.54056 Å) at 298 K. Zeta potential and relative hydrodynamic radius were estimated using dynamic light scattering on Nanotrac™ (Montgomeryville, PA, USA). Infrared spectra of synthesized PEG-8000 and mixed ceria (CeO_2-x) nanoparticles were performed using Fourier transform infrared spectrometer (Bruker; Billerica, MA, USA) fitted with KBr beam splitter, and deuterated triglycine sulfate/KBr detector. The spectra were recorded in the solid state in KBr pellets. In the employed configuration, it has been possible to cover the 400–4,000 cm⁻¹ range with a resolution of 4 cm⁻¹.

Imaging nanoparticles' internalization using TEM

Animals were fixed, perfused with 2% paraformaldehyde, and intact brains were collected. Hippocampus was microdissected and sectioned into 1×1 mm pieces and allowed to fix overnight in 2.5% gluteraldehyde. Further, tissues were embedded in aryldite resin, cut into 2 nm thin sections using ultramicrotome (Ultramicrotome EM UC7; Leica Microsystems, USA) and fixed on copper grids (Wetzlar, Germany). Grids were

analyzed under TEM (Technai G^2 Spirit; FEI, OR, USA) at a power of 120 keV and 15,000 magnification. Images were acquired and analyzed using TechnaiEPU automation software (Hillsboro, OR, USA). Presence of nanoceria was further confirmed with SAED pattern. A minimum of two grids per sample were analyzed with five different fields.

Estimation of oxidative stress markers

Estimation of several known markers of oxidative stress was performed immediately after microdissecting the hippocampus of rat brain. Estimation of ROS, malondialdehyde (MDA), carbonylation, protein oxidation, and DNA damage was performed as described later.

ROS estimation

ROS levels were measured with a nonfluorescent, lipophilic dye dichlorofluorescein diacetate that passively diffuses through cellular membranes where it is cleaved into 2,7-dichlorofluorescein by intracellular esterase enzymes in the presence of intracellular ROS; this reaction is known to be directly proportional to ROS levels. Exactly 10 μL of 10 μM 2′,7′-dichlorodihydrofluorescein diacetate was added to 150 μL of hippocampus tissue homogenate (10% w/v in Radioimmunoprecipitation assay buffer) and incubated for 40 minutes at 37°C in amber tubes in dark. Fluorescence was measured at 488 nm excitation and 525 nm emission (LS45 luminescence spectrophotometer; PerkinElmer Inc., Waltham, MA, USA) and converted to fluorescence units per milligram of protein.

Lipid peroxidation estimation

Lipid peroxidation was measured by direct estimation of MDA in hippocampus homogenate using the method suggested by Okahawa et al[32] with a slight modification. Briefly, 750 μL of trichloro acetic acid (TCA; 20% in distilled water) and 750 μL of thiobarbituric acid (0.67% in 0.05 M NaOH) were added to 250 μL tissue homogenate. The mixtures were incubated in a water bath at 85°C for 45 minutes. The mixture was then allowed to cool at room temperature, followed by centrifugation at 400× g for 5 minutes. Approximately 200 μL of the supernatant was removed and the absorbance was measured at 531 nm using a spectrophotometer (Vera Max microplate reader; Molecular Devices LLC, Sunnyvale, CA, USA). The values were expressed in μmoles/mg protein.

DNA damage: 8-hydroxydeoxyguanosine estimation

As a measure of DNA damage caused by ROS, 8-hydroxydeoxyguanosine (8-OHdG) was estimated using 8-OHdG competitive enzyme-linked immunosorbent assay kit (Cat# E-EL-0028; Elabsciences, Beijing, People's Republic of China) as per the manufacturer's instructions. Briefly, hippocampal tissue homogenate was prepared in cold PBS. Then 50 μL samples, standards, samples and blanks were mixed with biotinylated detection antibody to a 96 well plate in duplicate. The plate was incubated at 37°C for 45 minutes. After three washings with wash buffer, 100 μL of streptavidin–horseradish peroxidase conjugate was added to each well and again incubated at 37°C for 30 minutes. Furthermore, the plate was washed three times, and 90 μL of substrate solution was added and incubated at 37°C for 15 minutes in dark. Finally, 50 μL stop solution was added to each well, and the optical density was measured at 450 nm immediately. The concentration of 8-OHdG was measured using standard curve as described. Concentration was represented as ng/mg of protein.

Protein carbonylation estimation

Protein carbonylation assay was performed using protein carbonyl assay kit (Cayman Chemicals, Ann Arbor, MI, USA) as per the manufacturer's instructions. Briefly, 200 μL hippocampus tissue homogenate was added to 800 μL of 2,4-dinitrophenylhydrazine (DNPH). In the control tube was taken 800 μL of 2.5 M HCl. Both tubes were incubated in dark at room temperature for 1 hour. Then 1 mL of 20% TCA was added to each tube and incubated on ice for 5 minutes. Tubes were centrifuged at 10,000× g for 10 minutes at 4°C to pellet the protein. The pellet was resuspended in 1 mL of 10% TCA and incubated on ice for 5 minutes. The tubes were centrifuged at 10,000× g for 10 minutes, and the pellet was washed in 1:1 mixture of ethanol and ethyl acetate. Finally, the pellet was resuspended in 500 μL of guanidine hydrochloride and centrifuged at 10,000× g for 10 minutes. Then, 220 μL of the supernatant each from the sample tube and the control tube was loaded into microtiter plate and absorbance was measured at 370 nm. The carbonyl content was measured using molar absorption coefficient 22,000 M^{-1} cm^{-1} and expressed as picomoles per milligram of protein.

Protein oxidation using oxyblot

Protein oxidation was assessed using oxyblot protein oxidation kit (Millipore, Billerica, MA, USA) according to the manufacturer's protocol. Briefly, protein samples from each group were quantified and equal amount of protein was dispensed into two tubes, one derived with DNPH and the other underived. DNPH derivation was performed for 15 minutes, and the reaction was stopped using the neutralization solution. Then, derived and underived samples were loaded on 10% sodium dodecyl sulfate-polyacrylamide gel electrophoresis,

separated, and transferred to a nitrocellulose membrane. The nitrocellulose membrane was then blocked in 5% skimmed milk solution overnight at 4°C. The membrane was washed with PBS with 0.1% tween 20 and incubated with rabbit anti-DNPH antibody (1:150 dilution) for 2 hours. The membrane was again washed and incubated with anti-rabbit antibody (1:300 dilution) for 1.5 hours. Finally, results were acquired on X-ray film using chemiluminescent substrate (cat# CPS 1300-1KT). Underived samples transferred on the membrane were stained with Ponceau stain to visualize the protein bands. Further semiquantitation of the blots was performed using ImageJ (National Institute of Health, Bathesta, MD, USA) as described previously.[33]

MWM test

Hippocampal-dependent special cognition was tested in rats using standard MWM test as described earlier.[34] The water maze consisted of a circular pool (diameter 1.2 m, height 0.5 m) fitted with an overhead video recording device connected to a computer. Initially, the animals were habituated for 2 days by keeping them in the room containing MWM and leaving in water for 5 minutes. Then, for the next 8 days, acquisition trials were conducted by keeping the Plexiglas platform hidden below the surface of water. Position of platform was kept constant, but the start position for animals was varied. On the final day, control and PEG-CNPs animals were subjected to probe trial, and the remaining animals were exposed to 10-day hypoxia. Finally, the hypoxia and PEG-CNPs + hypoxia animals were subjected to a 2-day acquisition trial and a final probe trial. The results were acquired using a professional software package Anymaze v3.0 (Wood Dale, IL, USA). In the acquisition trial, the latency to reach the hidden platform, path tracks, and the time spent in each quadrant were calculated. While during the probe trial, the platform was removed and the time spent by the animals in the platform quadrant and the number of annulus crossings were measured.

Primary culture of adult rat hippocampus and flow cytometry

Animals from each group were euthanized, and brains were microdissected to obtain hippocampi. Hippocampal tissue mass was suspended in culture media (DMEM). Tissue was then triturated using fine needle syringe 18–20 times to obtain a homogeneous cell suspension. Suspension was then centrifuged at 1,500 rpm for 15 minutes to obtain the cells as a pellet. The cells were then washed with Dulbecco's PBS and plated on a poly-D-lysine precoated plate. The medium was changed after 24 hours on the first day and, subsequently, after 48 hours. Cells were grown in normal cell culture conditions

(37°C and 5% CO_2) in DMEM supplemented with 10% fetal bovine serum and penicillin/streptomycin. Bromodeoxyuridine was added to the culture media at a final concentration of 10 µM and incubated for 4 hours. Further, the cells were centrifuged, fixed, and permeabilized with Cytofix/Cytoperm Plus permeabilization buffer for 10 minutes at 4°C. Then, the cells were treated with 100 µL of DNase (300 µg/mL) for 1 hour at 37°C. Further, the cells were resuspended in 20 µL of BD Perm/Wash Buffer + Alexa Fluor 488 Anti-BrdU (cat# ab115874; Abcam, Cambridge, UK) and Alexa Fluor 647 Anti-NeuN (cat# ab190565; Abcam) antibodies for 20 minutes at room temperature. Finally, the cells were washed, and immunofluorescence measurements were performed on multicolor flow cytometer (LSR II; San Jose, CA, USA). Suitable single-color compensation controls and gating controls were also run in parallel. Data were analyzed with inbuilt software and presented as dot plot with quadrant statistics.

Cresyl violet staining

Cresyl violet staining was performed as described previously[35] with slight modifications. In brief, rats were perfused with cold PBS and perfuse fixed with 4% paraformaldehyde. Brains were excised and stored in 4% paraformaldehyde till the completion of fixation. Paraffin blocks were prepared and sectioned in 7 µm thickness and processed in cresyl violet staining. Morphology of neurons was then observed under the light microscope, and the relative number of pyramidal neuronal cells of hippocampus was estimated using RGB histogram function of ImageJ software (NIH, v3.0). A minimum of three sections per slide were obtained, and three animals per group were analyzed. Results were represented as mean density of positively stained cells.

Immunoblotting

Immunoblotting was performed using rabbit anti-AMPK, rabbit anti-pCBP, rabbit anti-pPKCζ, rabbit anti-cleaved caspase-3, and caspase-9 primary antibodies. Sodium dodecyl sulfate-polyacrylamide gel electrophoresis was used to separate proteins were then transferred to a nitrocellulose membrane using semidry western transfer equipment (GE Healthcare Bio-Sciences Corp., Piscataway, NJ, USA). The nitrocellulose membrane (cat# Z613657; Sigma-Aldrich Co., St Louis, MO, USA) was then incubated with blocking solution overnight at 4°C. The following day, it was incubated with primary antibody for 2 hours in a dilution of 1:2,000 and then in secondary antibody for 1 hour in a dilution of 1:10,000. Each step was preceded by three washings with PBS with 0.1% Triton X for 5 minutes. Finally, the blots were developed using chemiluminescent peroxidase

substrate, and signals were obtained on a photographic film (XBT film; Kodak, India). Images were acquired using gel documentation system. The relative densities of the protein bands were determined using ImageJ and expressed as number of pixels per group.

Statistical analysis

Performance on MWM test was analyzed using analysis of variance and simple comparisons between the groups were performed by unpaired Student's *t*-test with Mann–Whitney's post hoc analysis. Cumulative distances, time spent in each quadrant, and escape latency were acquired using Anymaze software and data were independently analyzed in MS Excel with statistical package add-in. In all the tests, the difference was considered significant with *P*-value <0.05. All the values were represented as mean ± standard error of mean unless specified.

Results

Synthesis and characterization of PEGylated nancoeria

CNPs were synthesized using aqueous hydrothermal method with PEG as the coating agent[23] and further subjected to extensive characterization before the experiment. Size and shape of the PEG-CNPs were analyzed using high-resolution TEM (HR-TEM), and the nanoparticles were observed as spherical heterogeneous mixture with a size range of 2–4 nm and averaging to 3 nm (Figure 2A and B). The purity of nanoparticles was assessed using XRD, and the XRD spectra showed prominent {111}, {200}, {044}, and {220} lattice indices that are characteristic of calcium fluorite structure, therefore confirming the purity of cerium oxide crystals used for the nanoparticle synthesis (Figure 2C). Further, to assess the stability of synthesized nanoparticles in aqueous

phase, we used dynamic light scattering and observed hydrodynamic radii of 40–45 nm (Figure 2D). Furthermore, the Fourier transform infrared spectra were obtained to assess the conjugation of PEG. Figure 2E shows the OH stretching vibrations of the free PEG-8000 modified from 3,465 cm^{-1} to a broad band centered approximately 3,387 cm^{-1}. The peak approximately at 3,481 cm^{-1} was assigned to Ce–O stretching vibration (Figure 2E).

PEGylated CNPs crossed blood–brain barrier and deposited in brain

After characterization of PEG-CNPs, we performed a qualitative analysis of internalization of these particles in the brain tissue 24 hours after the last dose and observed that electron-dense particles were scattered heterogeneously in the neuronal cells (Figure 3). The identity of the particles was further confirmed using SAED. Moreover, we also assessed the presence of particles in the tissue 30 days after the last dose and found decreased density of particles indicating histological clearing (Figure S1). The suspension of PEG-CNP in PBS at a concentration of 5 μg/kg body weight in successive three doses on a weekly basis was used in all the experiments, based on previous optimization regimes for primary neuronal culture and evidence from reports suggesting 0.1% deposition of injected formulation in brain.[36] The optimization of route was confirmed using radioactive Tc99 label-based imaging of internalized PEG-CNPs and evaluation using standard gamma scanning (Figure S1).

PEG-CNPs scavenged ROS en source and prevented biomolecule modification

Since CNPs possess inherent antioxidant activity, we evaluated the basal ROS levels and prominent markers of oxidative
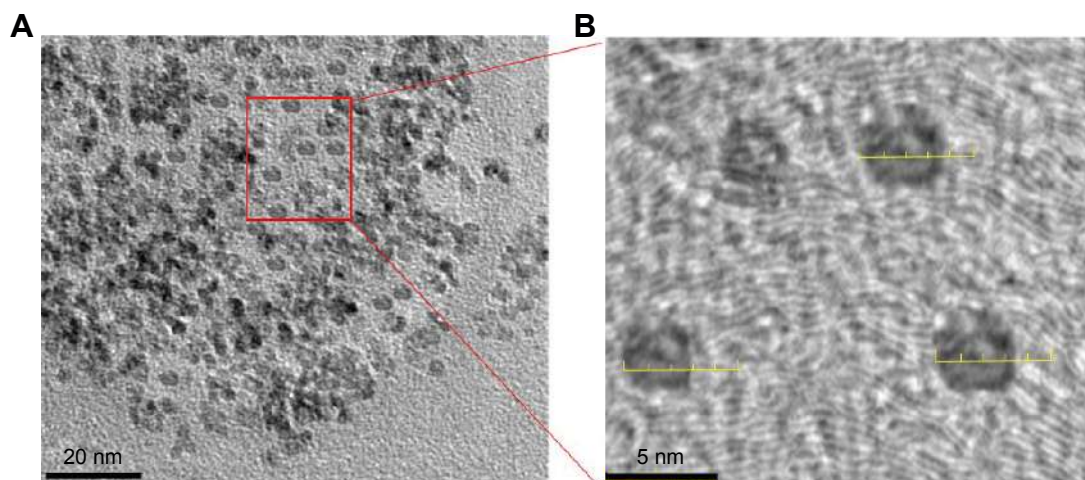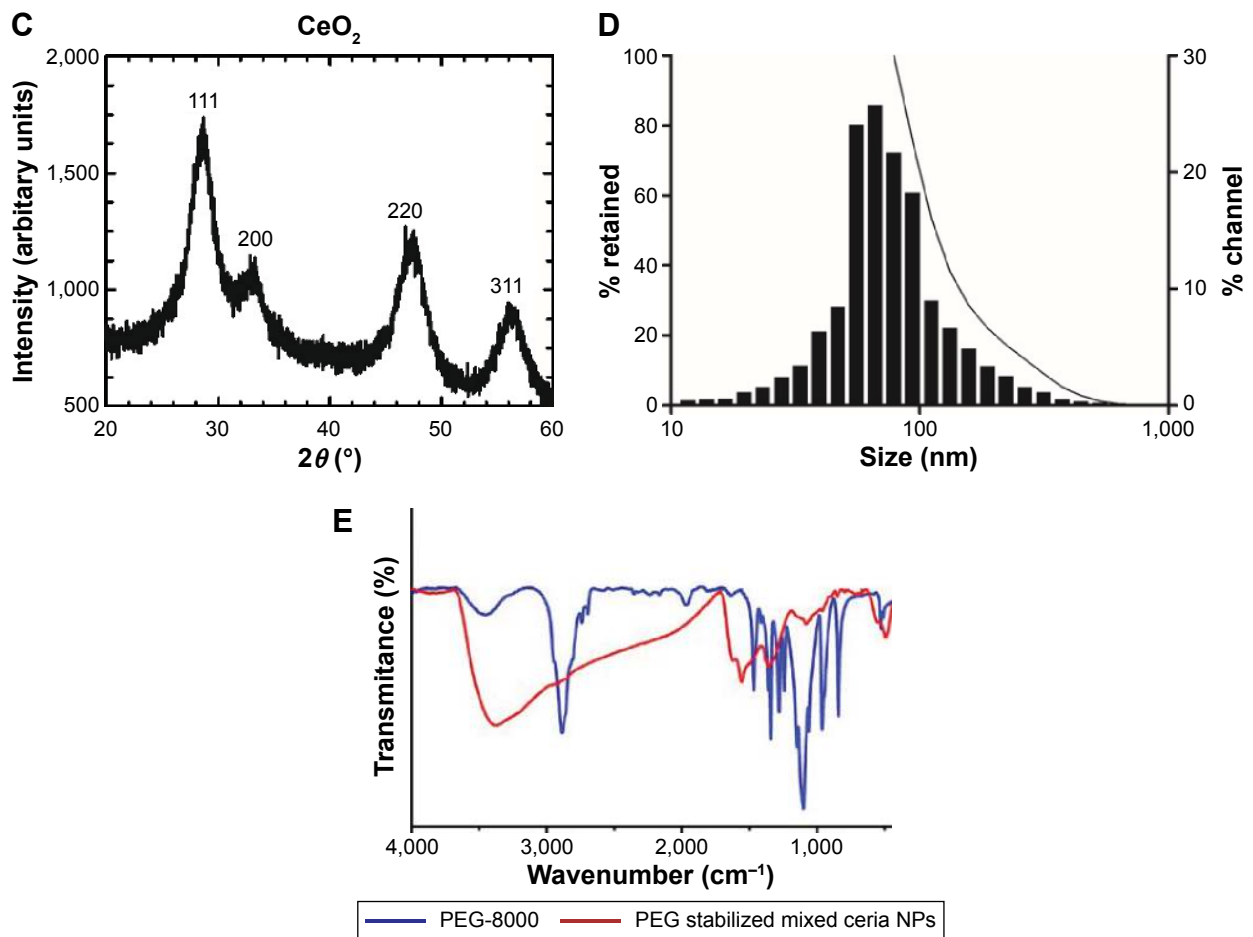

Figure 2 (*Continued*)

C CeO$_2$

Figure 2 Characterization of PEG-CNPs.
Notes: (**A**) Transmission electron micrographs of PEG-CNPs showing uniformly distributed spherical nanoparticles (scale bar: 20 nm). (**B**) Magnified view revealing diameter of PEG-CNPs in the size range of 3–5 nm. The selected area electron diffraction pattern confirms the ceria crystal structure in transmission electron microscopy. (**C**) X-ray diffraction analysis of the crystal lattice of PEG-CNPs showing prominent lattice planes {111}, {200}, and {220}. (**D**) Dynamic light scattering of CNPs in cerebrospinal fluid; mean hydrodynamic diameter was observed as 90 nm. (**E**) FT-IR spectra showing conjugation of PEG to CNPs.
Abbreviations: CNPs, cerium oxide nanoparticles; PEG, polyethylene glycol; NPs, nanoparticles.

damage in isolated homogenate of brain hippocampi. We observed that the concentration of ROS in the hypoxic animals was twofold higher in comparison to control animals, while PEG-CNPs animals subjected to hypoxia showed ROS levels similar to normoxic levels. Interestingly, PEG-CNP itself did not elevate ROS levels (Figure 4A). We also estimated oxidative stress parameters such as MDA content as an indicator of lipid peroxidation, 8-OHdG levels
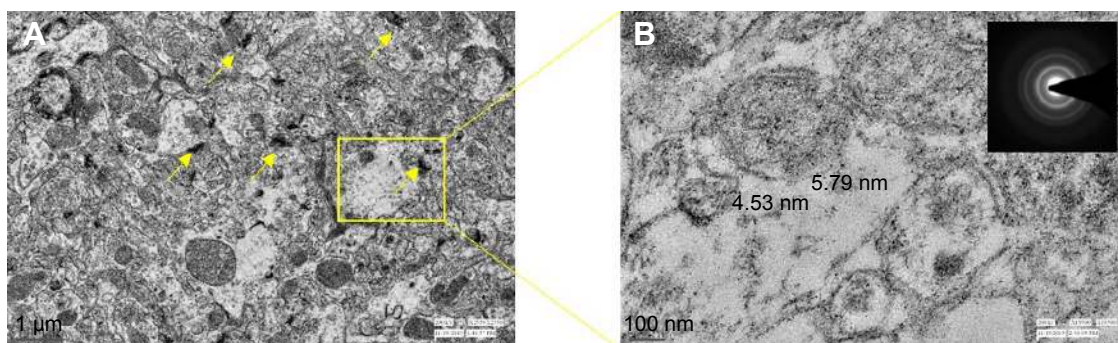

Figure 3 Assessment of polyethylene glycol-cerium oxide nanoparticles biodistribution using transmission electron microscopy.
Notes: Electron micrograph of rat brain hippocampus region. (**A**) The electron-dense nanoparticles of polyethylene glycol-cerium oxide nanoparticles were observed after 24 hours of third dose. Arrows indicate the presence of CNPs in the hippocampus. Scale bar: 1 μm. (**B**) Magnified view of nanoparticles is indicated with their size (~4–5 nm) and selected area electron diffraction with characteristic diffraction fringes (inset). Scale bar: 100 nm.
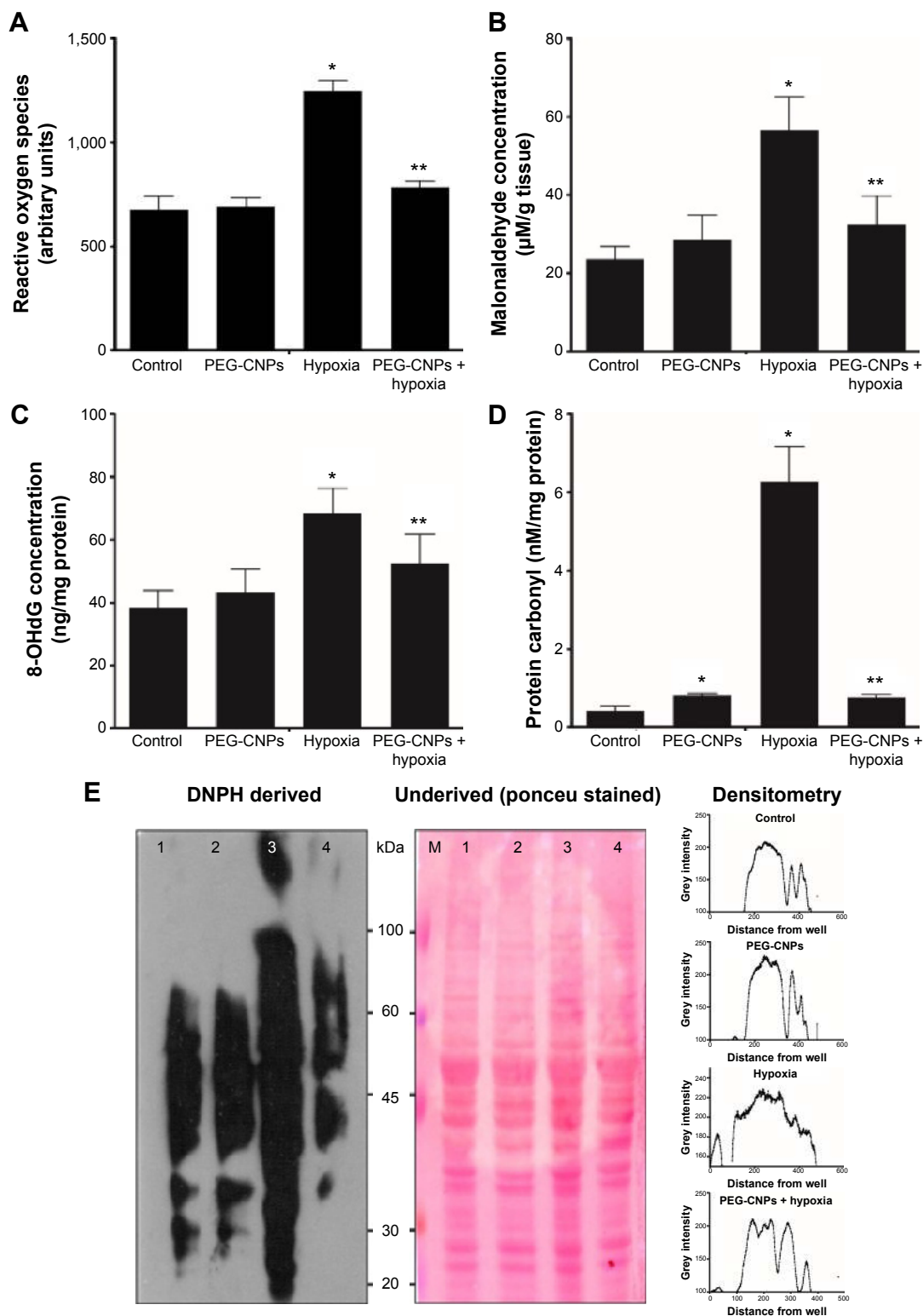**Abbreviation:** CNPs, cerium oxide nanoparticles.

Figure 4 Evaluation of oxidative stress in the hippocampus region of rat brain.
Notes: (**A**) ROS dichlorofluorescein diacetate fluorescence in arbitrary units as a measure of relative ROS content in the isolated rat hippocampi showed twofold higher ROS content in animals exposed to hypoxia. PEG-CNPs pretreatment significantly reduced the ROS content. Also, PEG-CNPs alone did not cause any increase in ROS. (**B**) MDA estimation using thiobarbituric acid reactive substances assay showed 2.4-fold higher MDA content in hypoxia, while PEG-CNPs pretreatment reduced the level of MDA to 1.4-fold in comparison to control. PEG-CNPs alone did not cause any elevation in MDA. (**C**) 8-OHdG concentration in animals exposed to hypoxia was 1.8-fold higher, while PEG-CNPs pretreatment in hypoxia reduced the concentration to 1.3-fold in comparison to control. PEG-CNPs alone did not elevate 8-OHdG. (**D**) Protein carbonylation estimation using enzyme-linked immunosorbent assay and (**E**) protein carbonylation estimation using oxyblot showed highest degree of protein carbonylation in hypoxia samples, while PEG-CNPs pretreatment prevented the carbonylation. Graphical view of immunoblot analyzed using ImageJ represents relative intensity at each level in the gel. Data represented as mean ± standard error of mean of three independent experiments (*$P<0.01$, **$P<0.05$).
Abbreviations: 8-OHdG, 8-hydroxydeoxyguanosine; CNPs, cerium oxide nanoparticles; MDA, malondialdehyde; PEG, polyethylene glycol; ROS, reactive oxygen species; DNPH, dinitrophenylhydrazine.

as a marker of nucleic acid damage, and levels of protein carbonylation. We observed that MDA content in normoxic animals was 23.5 ± 3.2 μM, while hypoxia increased the MDA content to 56.5 ± 8.4 μM. PEG-CNP pretreatment significantly prevented this elevation and restricted the MDA content to 34.5 ± 7.3 μM. PEG-CNPs alone showed no significant elevation in MDA content (Figure 4B). Similarly, 8-OHdG levels were 38.4 ± 5.4 ng/mg tissue in normoxic condition, which elevated to 68.4 ± 7.9 ng/mg in hypoxia, while PEG-CNPs pretreatment reduced the level to 52.4 ± 9.3 ng/mg (Figure 4C). It is important to note that extensive protein carbonylation levels (more than 12-fold) were observed in hypoxic animals. The carbonyl content in normoxia was 0.4 ± 0.1 nM but increased to 6.27 ± 0.9 nM in hypoxia. PEG-CNPs pretreatment during hypoxia effectively reduced this to 0.76 ± 0.07 nM (Figure 4D). Further, we also confirmed the protein carbonylation levels using Western blot-based oxyblot technique and analyzed the results with ImageJ software (NIH, v3.0). The oxyblot results further revealed higher protein carbonyl content in hypoxic brain homogenate as compared to normoxic animals. The PEG-CNP pretreated animals exhibited significantly reduced

levels of protein carbonyls post-hypoxia, corroborating the in vitro antioxidant potential of nanoceria (Figure 4E).

PEG-CNPs improve cognition in rat during chronic hypobaric hypoxia

Animal studies have reported that chronic hypobaric hypoxia exposure results in memory impairment and loss of neuronal viability.[8,12] We have previously reported the antioxidant and antiapoptotic roles of CNPs in primary neuronal culture during oxidative stress.[37] In the present study, we have evaluated the neuroprotective roles of PEG-CNPs in protecting rodent brain, specifically cognition, during chronic hypobaric hypoxia. Using the conventional MWM spatial memory assay, we evaluated the abrogation of memory impairment after 10 days of hypobaric hypoxia. Latency to reach the hidden platform was used as an indication of learning abilities in animals. On comparing normoxic controls with PEG-CNPs treated animals, we observed an improved cognition in the latter. Furthermore, on subjecting both these groups to hypobaric hypoxia for 7 days, we observed a significant memory loss in the untreated animals, while PEG-CNPs pretreated animals showed early recovery and responded to spatial learning (Figure 5A).
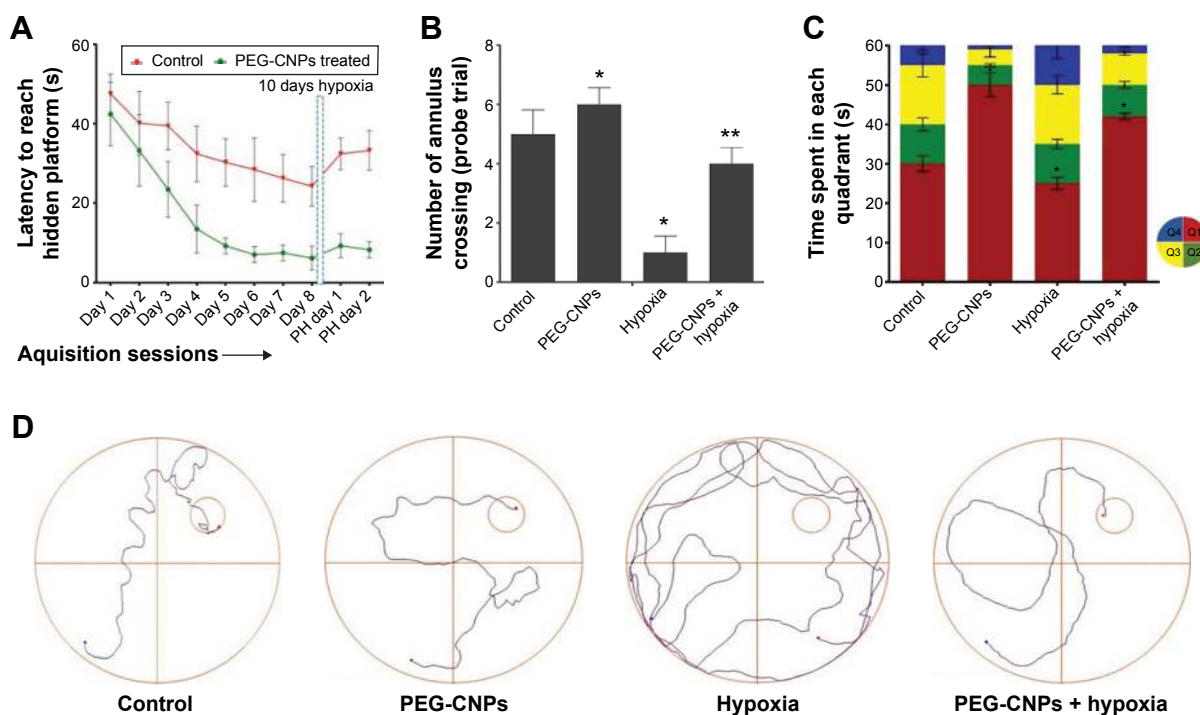

Figure 5 Evaluation of spatial memory in rat after PEG-CNPs intervention.
Notes: Spatial memory function test in rat using Morris water maze. (**A**) Graph showing latency to reach the hidden platform. Steeper slope in animals treated with PEG-CNPs, compared to controls indicated better retention of spatial memory. After hypoxia, the increase in latency was smaller in PEG-CNPs pretreated animals as compared to hypoxic animals. (**B**) Number of annulus crossings during the probe trial. Control animals showed five times mean annulus crossing, PEG-CNP treated animals showed six times, hypoxia-exposed animals showed only one annulus crossing, and PEG-CNPs + hypoxia animals showed four time annulus crossing. (**C**) Analysis of time spent in each quadrant during the probe trial showed that PEG-CNPs treated animals spent maximum time in target quadrant which was 40% higher than control, while minimum time was observed in animals subjected to hypoxia, which was 20% less than control; PEG-CNPs + hypoxia group spent 30% more time compared to control (*$P<0.05$, **$P<0.01$ Q1 – target quadrant containing hidden platform). (**D**) Representative path tracks of animals during spatial acquisition trials.
Abbreviations: CNPs, cerium oxide nanoparticles; PEG, polyethylene glycol.

On the final day during the probe test, the number of annulus crossings were also higher in case of animals pretreated with PEG-CNPs in comparison to hypoxic animals (Figure 5B). Similarly, the time spent by rats in the platform quadrant was minimum for hypoxic animals, but PEG-CNPs pretreated animals showed a higher fraction of time spent in Q1 (Figure 5C). Representative path tracks are shown in Figure 4D, which indicate increased travel distance in animals exposed to probe trial after hypobaric hypoxia exposure and a significant recovery in the animals pretreated with PEG-CNPs (Figure 5D). Associated media files containing CCD track records of rats during the probe trial have been enclosed as media files in: Control (Video S1), CNPs (Video S2), Hypoxia (Video S3), and Hypoxia + CNPs (Video S4).

PEG-CNPs promoted adult hippocampal neuron survival

In the present study, we also observed enhanced cognition in PEG-CNP-treated normoxic animals (Figure 5A) along with hypoxia-exposed animals during MWM tests. We next evaluated the neurogenesis patterns of PEG-CNP treated animals by culturing the adult hippocampus neurons to assess the effect of PEG-CNPs in improving the memory functions. Microscopic observations revealed that the neurons cultured from animals treated with PEG-CNPs showed higher neuronal density compared with the neurons cultured from hypoxia-exposed animals. On performing relative image quantification using ImageJ, we observed a 20% increase in the cell density in PEG-CNPs group, which was reduced
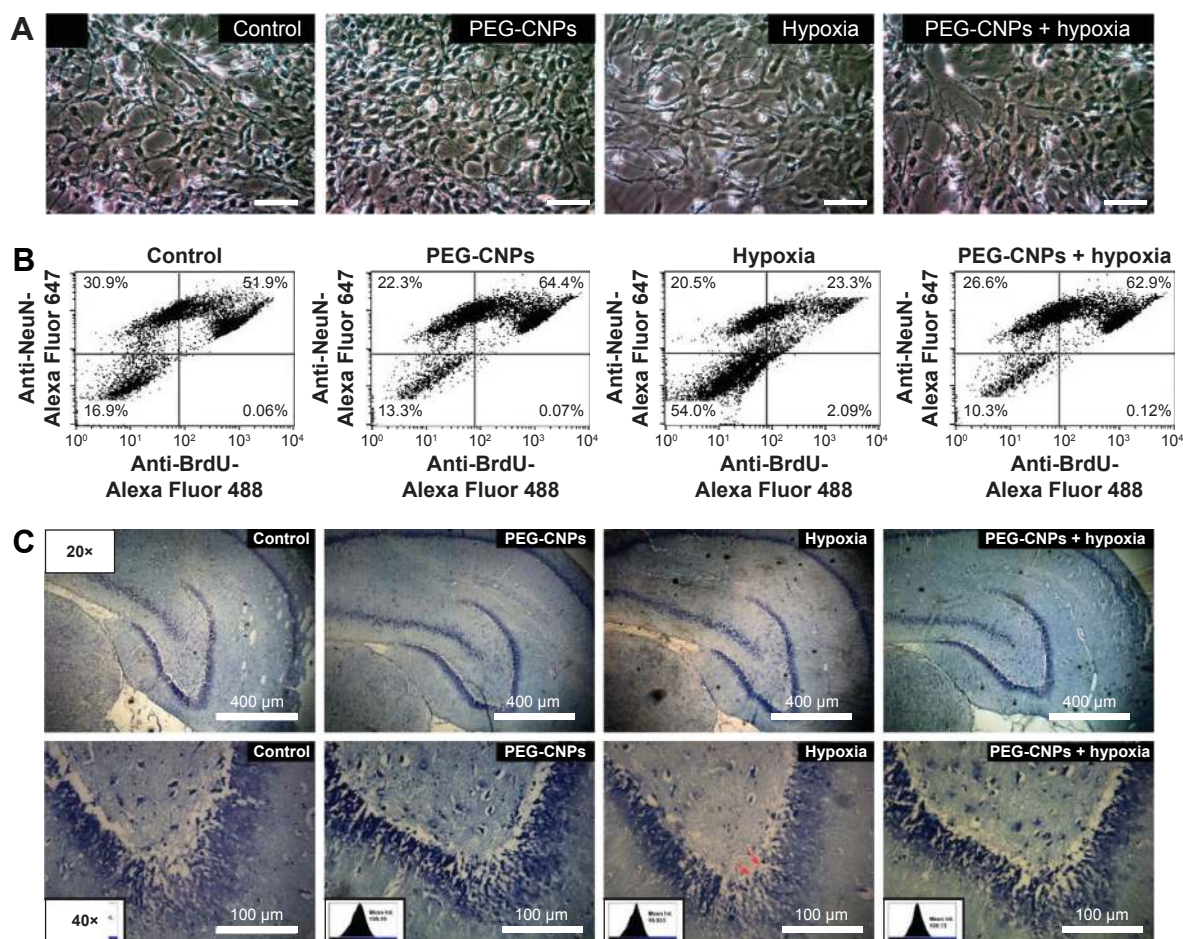

Figure 6 PEG-CNPs prevented apoptosis and induced neurogenesis.
Notes: (**A**) Phase-contrast microphotographs showing reduced number of neurons in hypoxia-exposed animals and increased density of neurons in PEG-CNP treated cells exposed to hypoxia (scale bar: 20 μm). (**B**) Dot plots showing the neuronal population with BrdU incorporation. Lower left quadrant represents neuronal nonproliferating cells, lower right quadrant represents nonproliferating neuronal cells, upper left quadrant shows neuronal nonproliferating cells, and upper right quadrant shows neuronal proliferating cells. There were 51.95 BrdU-positive neuronal cells in the control group, 64.4% in PEG-CNPs group, 23.3% in hypoxia group, and 62.9% in PEG + hypoxia group. (**C**) Photomicrographs of dentate gyrus region of rat hippocampus stained with cresyl violet show neurodegeneration, while neuron density was higher in PEG-CNPs treated animals. At higher magnification, the number of pyramidal cells (deep violet stained) was higher in PEG-CNPs treated cells. Insets represent the histograms of blue channel with mean values representing relative number of cresyl violet positive cells (control – 107.5, PEG-CNPs – 109.19, hypoxia – 98.93, PEG-CNPs + hypoxia – 109.13). Arrows indicate neurodegeneration.
Abbreviations: CNPs, cerium oxide nanoparticles; PEG, polyethylene glycol.

by 30% in hypoxia group in comparison to control. PEG-CNP + hypoxia also showed an increase in the cell density by 10% when compared to control (Figure 6A). Next, we confirmed neurogenesis using the BrdU incorporation into the neuronal cells (with neuron-specific marker NeuN) using flow cytometry. We observed that there were 51.9% BrdU-positive neuronal cells in the control group, 64.4% in PEG-CNPs group, 23.3% in hypoxia group, and 62.9% in PEG + hypoxia group. This indicated that PEG-CNPs promoted hippocampal neurogenesis in normoxia as well as in hypoxic condition, concomitant with improvement in the cognitive functions (Figure 6B).

Furthermore, neurogenesis was confirmed by cresyl violet staining of paraffin sections of PEG-CNP treated normoxic as well as hypoxic brains. We observed dense staining of pyramidal neurons in the dentate gyrus region of hippocampus of PEG-CNP treated normoxic and hypoxic brains as compared to normoxic brains, further corroborating neurogenesis (Figure 6C). These cumulative results suggest that PEG-CNPs promote neurogenesis in rat brain, irrespective of the oxygen availability.

Nanoceria regulate AMPK–PKC–CBP axis for neurogenesis

Our previous studies along with other studies have reported the abilities of nanoceria in modulating mitochondrial functions and bioenergetics.[37,38] In the present study, we evaluated the expression levels of AMPK and downstream regulators PKC and CBP central to neurogenesis by western blotting. We observed significantly higher levels of AMPK in hypoxia + CNPs group (Figure 7). Interestingly, AMPK activates a molecular cascade via nuclear histone acyltransferase protein CBP and PKC, directing the adult neurogenesis.[39] PEG-CNPs treatment also increased the amount of phosphorylated aPKCζ and further activated the CBP by phosphorylation (Figure 7). Conventionally, AMPK–CBP axis is involved in regulation of glucose metabolism in the liver, but a relatively new route has been recently reported in neuronal cells where activated pCBP is involved in adult neurogenesis.[39] These observations further support abrogation of hypoxia-induced memory impairment by PEG-CNPs intervention. Concomitantly, we observed significant decrease in the expression of apoptosis-associated proteins caspase-3 and caspase-9 in PEG-CNPs pretreated hypoxic hippocampus as compared to hypoxic hippocampus (Figure 7). These results provide indirect evidences for enhanced survival of PEG-CNP pretreated hippocampal tissue during hypoxia.
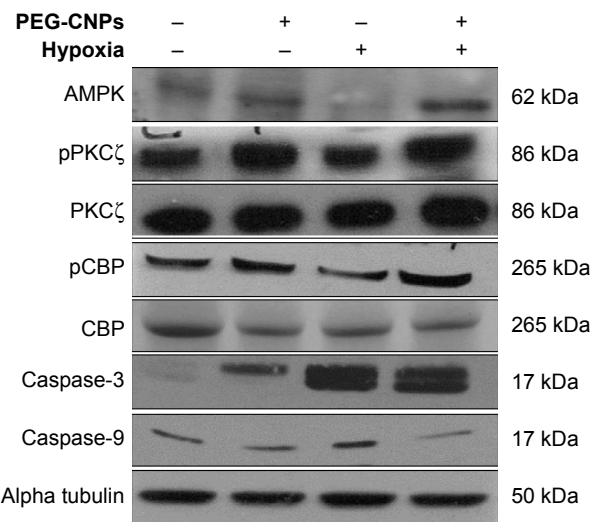

PEG-CNPs	–	+	–	+	
Hypoxia	–	–	+	+	
AMPK					62 kDa
pPKCζ					86 kDa
PKCζ					86 kDa
pCBP					265 kDa
CBP					265 kDa
Caspase-3					17 kDa
Caspase-9					17 kDa
Alpha tubulin					50 kDa

Figure 7 Evaluation of key molecular targets of PEG-CNPs using immunoblotting.
Notes: Immunoblots show changes in expression or phosphorylation of neurogenic and apoptotic markers in the rat brain homogenates. AMPK expression was increased after PEG-CNPs treatment, while it was reduced in hypoxic exposure. Further, it was the highest in PEG-CNPs group. Phosphorylation of PKCζ and pCBP was increased in both PEG-CNPs and hypoxia + PEG-CNPs groups, while decreased phosphorylation was observed in hypoxia group compared with control. Caspase-3 and caspase-9 (cleaved forms) were upregulated in hypoxia alone, while PEGylated-CNP treatment reduced the concentration of both in comparison to control. Alpha tubulin was used as the loading control for all samples.
Abbreviations: AMPK, 5′-adenine monophosphate-activated protein kinase; CBP, cyclic adenosine monophosphate response element-binding protein binding protein; CNPs, cerium oxide nanoparticles; PEG, polyethylene glycol; PKC, protein kinase C.

Discussion

The present study reports the neurogenic and memory impairment ameliorating activities along with antioxidant activities of nanoceria during chronic hypoxia in rodent brain. Both human and animal studies have provided evidences for enhanced oxidative stress and damage as well as memory impairment during chronic hypobaric hypoxia. Since the brain regions such as hippocampus and cortex are deficient in antioxidant enzymes and rich in transition metals such as iron and copper, the degree of oxidative damage is more severe for these regions. Unfortunately, the conventional neuroprotective drugs find limited clinical applications due to limited brain penetration. With the advantages of brain targeting without blood–brain barrier (BBB) disruption[40] and specific coatings for long retention in brain,[25,26,30] nanoparticles are emerging as promising antioxidants as well as drug carriers for neuronal diseases. Using PEG-coated CNPs that are uniform with a size of 3 nm, Kim et al[6,25] have reported protection against ischemic stroke by reducing ROS and apoptosis. Similarly, CNPs with PEG as well as citrate/EDTA coatings have been used for free radical scavenging and specific targeting to amyloid beta (Aβ) aggregates.[27] In the present study, we extend the usage of

PEG-CNPs for neurogenesis-promoting as well as memory impairment abrogating activities, along with antioxidant and antiapoptotic activities during long-term hypobaric hypoxia. Moreover, the coating of PEG on nanoparticle did not cause any significant loss of antioxidant activity or any change in the surface properties (Figure S2).

Effective brain penetration without disrupting BBB has been reported for nanoparticles with <10 nm particle diameter. Moreover, naked nanoparticles are rapidly engulfed by macrophages and cleared from the body before reaching targets.[24,41] A dense coating of PEG on particles of small size (≤10 nm) has been reported for effective brain targeting and diffusion within the brain tissue.[29,30] In the present study, we synthesized 3 nm spherical CNPs with PEG coating for effective brain localization.[25] Using a combination of TEM and radioactivity-based imaging, we observed efficient brain localization of PEG-CNPs in brain after 2 hours of intraperitoneal injection. Interestingly, this mode of injection also resulted in heart localization of PEG-CNPs. In contrast, the same dose of PEG-CNPs administered though oral or IV route does not localize in brain and heart, suggesting that the route of administration also plays an important role in tissue localization of nanoparticles. Our present study also suggests that PEG-CNPs with <5 nm size efficiently cross the BBB and localize in the brain.[27,29,42]

PEG-coated CNPs exhibit excellent stability and disparity in physiological solutions, as well as efficiently quench noxious free radicals and peroxides mimicking superoxide dismutase activity, as compared to bare CNPs.[42,43] Hence, we evaluated the in vivo antioxidant activities and the level of oxidative modification of proteins after 10 days of hypobaric hypoxia exposure. This hypoxia exposure reportedly elevates brain ROS levels resulting in oxidative damage, as well as leads to memory impairment.[8,44] PEG-CNP pretreatment resulted in significant decrease in ROS levels, MDA content, as well as protein carbonyl content, as compared to hypoxic brain. Similarly, the protein oxidation levels were also lower in pretreated animals, further supporting in vivo antioxidant potential of PEG-CNPs.[42] Next, we evaluated the expression levels of caspase-9, an initiator caspase, and caspase-3, an effector caspase, which mediate the terminal stages of neuronal apoptosis.[45] Higher levels of both caspase-9 and caspase-3 were observed in hypoxia-exposed group, whereas a significant reduction of both proteins was observed in PEG-CNP pretreated and hypoxia-exposed animals. During transient global ischemia, loss of mitochondrial barrier function results in the release of caspase-9 from the mitochondria, which further accumulates

in the nucleus of hippocampal neurons preceding apoptosis.[46] This mitochondrial membrane permeabilization is a decisive step for cellular survival and death and is a pharmacological target for prevention of unwarranted cell death.[47] We have previously reported that CNPs stabilize mitochondrial membrane potential and prevent apoptosis during hypoxia in primary cortical culture.[37,48] The results of the present study showing lower expression of caspase-3 and caspase-9 with brain homogenates of PEG-CNP pretreated animals can be attributed to the mitochondrial membrane permeabilization and, thus, the antiapoptotic activities of nanoceria.

In vitro studies have reported that CNPs confer neuroprotection to adult rat spinal cord neurons[23] as well as primary cortical neuron cultures,[37] primarily by scavenging the free radicals. Using in vitro and in vivo models, Kim et al[25] have reported that 3 nm PEG-coated CNPs scavenge ROS, reduce apoptosis, and confer neuroprotection during ischemic stroke. Similar studies with murine model of multiple sclerosis have reported mitigation of ROS-induced tissue damage and alleviation of clinical symptoms and motor deficits by IV injection of CNPs.[26] In their study on the neuroprotective efficacy of CNPs, Dowding et al[27] have also reported that CNPs prevent neuronal cell death during Alzheimer's disease by reducing endogenous peroxynitrite levels and Aβ-induced mitochondrial fragmentation. In corroboration, our observed results of lower levels of free radicals and oxidative modified macromolecules, along with salvation of memory during chronic oxidative stress emphasize the neuroprotective efficacy of PEG-CNPs.

The lifelong generation of new neurons in the dentate gyrus region of the hippocampus is sustained due to proliferation and differentiation of adult neural stem cells.[14,49,50] The integration of these neurons into the circuitry of the adult hippocampus suggests an important role for adult hippocampal neurogenesis in learning and memory.[14] Since PEG-CNP pretreated animals performed better in MWM task after hypoxia exposure, we evaluated the neurogenesis patterns of both hypoxic and PEG-CNP pretreated hypoxic brains. Microscopic examination of cultured adult hippocampus neurons suggested higher neuronal density in PEG, thus providing evidence for neurogenesis-promoting activities of nanoceria which might have contributed to improved cognition after hypoxic challenge.[15,16] Activation of CREB stimulates neurogenesis in adult dentate gyrus.[51] Recent studies suggest AMPK–CREB axis represents an evolutionarily conserved pathway in response to low energy availability.[52,53] Moreover, activation of AMPK pathway also regulates neuronal structure in developing hippocampal neurons.[54]
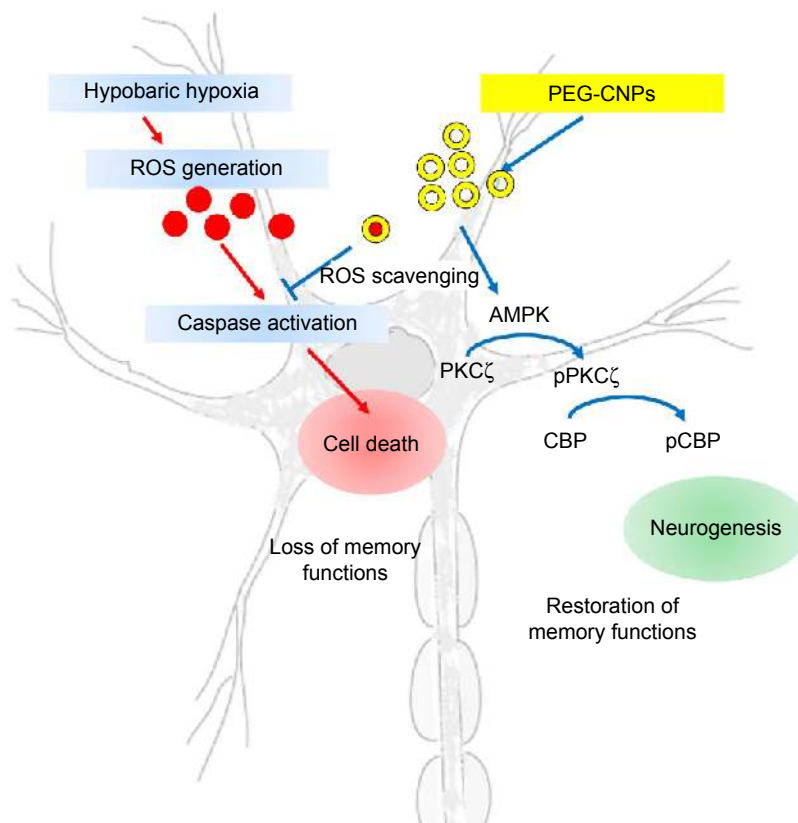
Figure 8 Mechanism of hippocampal neurogenesis and cell survival by PEG-CNPs.
Notes: AMPK activates a molecular cascade via nuclear histone acyltransferase protein CBP and PKC, directing the adult neurogenesis. PEG-CNPs treatment also increased the amount of phosphorylated aPKCζ and further activated CBP by phosphorylation, thereby activating adult hippocampal neurogenesis. Another route that operated during hypoxia was activation of apoptotic events mediated via caspase-3 and caspase-9, which was also inhibited by PEG-CNPs pretreatment.
Abbreviations: AMPK, 5′-adenine monophosphate-activated protein kinase; CBP, cyclic adenosine monophosphate response element-binding protein binding protein; CNPs, cerium oxide nanoparticles; PEG, polyethylene glycol; PKC, protein kinase C; ROS, reactive oxygen species.

We observed higher expression of AMPK in PEG-CNP pretreated brain homogenates. Since phosphorylation of the transcriptional coactivator CBP by PKC at serine 436 is critical for the physiological effects of CREB,[55] we also measured the phosphorylation status of both CBP and PKC. Along with AMPK, we also observed higher levels of pCBP and pPKC in PEC-CNP pretreated brain homogenates, as compared to that in hypoxic brains. It is important to note that CNPs possess inherent cellular signaling activities,[56] apart from their widely reported antioxidant activities. In their study on PEG-coated and anti-Aβ antibody-conjugated CNPs, Cimini et al[57] have reported modulation of brain-derived neurotrophic factor pathway promoting neuronal survival. Future use of omics technologies may identify the cell signaling potentials of nanoceria.

The present study has limitations of using Tc99-labeled CNPs for imaging studies. Due to short half-life of Tc99 label, we were not able to track the particles beyond 24 hours, and therefore, an alternative label should be used to further establish the pharmacokinetics. Moreover, we have not

quantified the accumulation and persistence of PEG-CNPs in rodent brain as well as in brain regions. In their study on similar-sized (2.9 nm diameter) citrate/EDTA CNPs, Heckman et al[26] have reported higher plasma half-life, and tolerance, and brain accumulation in animal models. Moreover, PEG-coated CNPs as large as 114 nm in diameter can diffuse though brain extracellular spaces at appreciable rates.[30] These studies tend us to speculate that PEG-CNPs used in this study can accumulate throughout the brain, warranting future experimental evidence.

In conclusion, the results of the present study with 3-nm-diameter PEG-coated CNPs extend the usage of CNPs in preventing memory loss during severe oxidative stress. Concomitantly, the study also provides evidence that PEG-CNPs promote neurogenesis by AMPK–PKC–CBP pathway (Figure 8). The observed neurogenesis-promoting activities along with previously reported neuroprotective efficacy of nanoceria during Alzheimer's disease and multiple sclerosis suggest the potential of nanoceria as a promising therapeutics for neuronal degenerative disorders.

Acknowledgments

Disclosure

References

1. Sharp FR, Bernaudin M. HIF1 and oxygen sensing in the brain. *Nat Rev Neurosci*. 2004;5(6):437–448.
2. Wilson MH, Newman S, Imray CH. The cerebral effects of ascent to high altitudes. *Lancet Neurol*. 2009;8(2):175–191.
3. LaManna JC, Chavez JC, Pichiule P. Structural and functional adaptation to hypoxia in the rat brain. *J Exp Biol*. 2004;207(Pt 18):3163–3169.
4. Zhang J, Yan X, Shi J, Gong Q, Weng X, Liu Y. Structural modifications of the brain in acclimatization to high-altitude. *PLoS One*. 2010; 5(7):e11449.
5. Zhang J, Zhang H, Li J, et al. Adaptive modulation of adult brain gray and white matter to high altitude: structural MRI studies. *PLoS One*. 2013;8(7):e68621.
6. Kim JW, Tchernyshyov I, Semenza GL, Dang CV. HIF-1-mediated expression of pyruvate dehydrogenase kinase: a metabolic switch required for cellular adaptation to hypoxia. *Cell Metab*. 2006;3(3): 177–185.
7. Papandreou I, Cairns RA, Fontana L, Lim AL, Denko NC. HIF-1 mediates adaptation to hypoxia by actively downregulating mitochondrial oxygen consumption. *Cell Metab*. 2006;3(3):187–197.
8. Maiti P, Singh SB, Sharma AK, Muthuraju S, Banerjee PK, Ilavazhagan G. Hypobaric hypoxia induces oxidative stress in rat brain. *Neurochem Int*. 2006;49(8):709–716.
9. Dosek A, Ohno H, Acs Z, Taylor AW, Radak Z. High altitude and oxidative stress. *Respir Physiol Neurobiol*. 2007;158(2–3):128–131.
10. Hota SK, Barhwal K, Singh SB, Ilavazhagan G. Differential temporal response of hippocampus, cortex and cerebellum to hypobaric hypoxia: a biochemical approach. *Neurochem Int*. 2007;51(6–7):384–390.
11. Sharma NK, Sethy NK, Bhargava K. Comparative proteome analysis reveals differential regulation of glycolytic and antioxidant enzymes in cortex and hippocampus exposed to short-term hypobaric hypoxia. *J Proteomics*. 2013;79:277–298.
12. Maiti P, Muthuraju S, Ilavazhagan G, Singh SB. Hypobaric hypoxia induces dendritic plasticity in cortical and hippocampal pyramidal neurons in rat brain. *Behav Brain Res*. 2008;189(2):233–243.
13. Turner E. Hippocampus and memory. *Lancet*. 1969;2(7630): 1123–1126.
14. Deng W, Aimone JB, Gage FH. New neurons and new memories: how does adult hippocampal neurogenesis affect learning and memory? *Nat Rev Neurosci*. 2010;11(5):339–350.
15. Nakashiba T, Cushman JD, Pelkey KA, et al. Young dentate granule cells mediate pattern separation, whereas old granule cells facilitate pattern completion. *Cell*. 2012;149(1):188–201.
16. Clelland CD, Choi M, Romberg C, et al. A functional role for adult hippocampal neurogenesis in spatial pattern separation. *Science*. 2009; 325(5937):210–213.
17. Heckert EG, Karakoti AS, Seal S, Self WT. The role of cerium redox state in the SOD mimetic activity of nanoceria. *Biomaterials*. 2008; 29(18):2705–2709.
18. Korsvik C, Patil S, Seal S, Self WT. Superoxide dismutase mimetic properties exhibited by vacancy engineered ceria nanoparticles. *Chem Commun (Camb)*. 2007;(10):1056–1058.
19. Pirmohamed T, Dowding JM, Singh S, et al. Nanoceria exhibit redox state-dependent catalase mimetic activity. *Chem Commun (Camb)*. 2010;46(16):2736–2738.
20. Xu C, Qu X. Cerium oxide nanoparticle: a remarkably versatile rare earth nanomaterial for biological applications. *NPG Asia Mater*. 2014;6(e90):1.
21. Ying X, Qingfen L, Dan Y, Xin Y, Kebin Z. Direct evidence for hydroxyl radical scavenging activity of cerium oxide nanoparticles. *J Phys Chem C*. 2011;115(11):4433–4438.
22. Singh S, Dosani T, Karakoti AS, Kumar A, Seal S, Self WT. A phosphate-dependent shift in redox state of cerium oxide nanoparticles and its effects on catalytic properties. *Biomaterials*. 2011;32(28): 6745–6753.
23. Das M, Patil S, Bhargava N, et al. Auto-catalytic ceria nanoparticles offer neuroprotection to adult rat spinal cord neurons. *Biomaterials*. 2007; 28(10):1918–1925.
24. Estevez AY, Pritchard S, Harper K, et al. Neuroprotective mechanisms of cerium oxide nanoparticles in a mouse hippocampal brain slice model of ischemia. *Free Radic Biol Med*. 2011;51(6):1155–1163.
25. Kim CK, Kim T, Choi IY, et al. Ceria nanoparticles that can protect against ischemic stroke. *Angew Chem Int Ed Engl*. 2012;51(44): 11039–11043.
26. Heckman KL, DeCoteau W, Estevez A, et al. Custom cerium oxide nanoparticles protect against a free radical mediated autoimmune degenerative disease in the brain. *ACS Nano*. 2013;7(12):10582–10596.
27. Dowding JM, Song W, Bossy K, et al. Cerium oxide nanoparticles protect against Abeta-induced mitochondrial fragmentation and neuronal cell death. *Cell Death Differ*. 2014;21(10):1622–1632.
28. Self WT, Bossy-Wetzel E, Seal S, Dowding J. Neuronal protection by cerium oxide nanoparticles. Google Patents. 2013.
29. Calvo P, Gouritin B, Brigger I, et al. PEGylated polycyanoacrylate nanoparticles as vector for drug delivery in prion diseases. *J Neurosci Methods*. 2001;111(2):151–155.
30. Nance EA, Woodworth GF, Sailor KA, et al. A dense poly(ethylene glycol) coating improves penetration of large polymeric nanoparticles within brain tissue. *Sci Transl Med*. 2012;4(149):149ra119.
31. Lee SS, Song W, Cho M, et al. Antioxidant properties of cerium oxide nanocrystals as a function of nanocrystal diameter and surface coating. *ACS Nano*. 2013;7(11):9693–9703.
32. Ohkawa H, Ohishi N, Yagi K. Assay for lipid peroxides in animal tissues by thiobarbituric acid reaction. *Anal. Biochem*. 1979;95(2): 351–358.
33. Arya A, Gangwar A, Sharma NK, Sethy NK, Bhargava K. Computational method for semi-quantitative analysis of immunoblots of modified proteins using ImageJ. *J Prot Proteomics*. 2015;6(3):10.
34. Vorhees CV, Williams MT. Morris water maze: procedures for assessing spatial and related forms of learning and memory. *Nat Protoc*. 2006;1(2):848–858.
35. Pilati N, Barker M, Panteleimonitis S, Donga R, Hamann M. A rapid method combining Golgi and Nissl staining to study neuronal morphology and cytoarchitecture. *J Histochem Cytochem*. 2008;56(6): 539–550.
36. Yokel RA, Tseng MT, Dan M, et al. Biodistribution and biopersistence of ceria engineered nanomaterials: size dependence. *Nanomed Nanotech Biol Med*. 2013;9(3):398–407.

37. Arya A, Sethy NK, Das M, et al. Cerium oxide nanoparticles prevent apoptosis in primary cortical culture by stabilizing mitochondrial membrane potential. *Free Radic Res*. 2014;48(7):784–793.

38. Arya A, Sethy NK, Singh SK, Das M, Bhargava K. Cerium oxide nanoparticles protect rodent lungs from hypobaric hypoxia-induced oxidative stress and inflammation. *Int J Nanomedicine*. 2013;8: 4507–4520.

39. Potts MB, Lim DA. An old drug for new ideas: metformin promotes adult neurogenesis and spatial memory formation. *Cell Stem Cell*. 2012; 11(1):5–6.

40. Yemisci M, Caban S, Gursoy-Ozdemir Y, et al. Systemically administered brain-targeted nanoparticles transport peptides across the blood-brain barrier and provide neuroprotection. *J Cereb Blood Flow Metab*. 2015;35(3):469–475.

41. McMillan J, Batrakova E, Gendelman HE. Cell delivery of therapeutic nanoparticles. *Prog Mol Biol Transl Sci*. 2011;104:563–601.

42. Karakoti AS, Singh S, Kumar A, et al. PEGylated nanoceria as radical scavenger with tunable redox chemistry. *J Am Chem Soc*. 2009;131(40): 14144–14145.

43. Li H, Yang ZY, Liu C, et al. PEGylated ceria nanoparticles used for radioprotection on human liver cells under gamma-ray irradiation. *Free Radic Biol Med*. 2015;87:26–35.

44. Magalhães J, Ascensão A, Soares JM, et al. Acute and severe hypobaric hypoxia increases oxidative stress and impairs mitochondrial function in mouse skeletal muscle. *J Appl Physiol (1985)*. 2005;99(4): 1247–1253.

45. Cowan CM, Thai J, Krajewski S, et al. Caspases 3 and 9 send a pro-apoptotic signal from synapse to cell body in olfactory receptor neurons. *J Neurosci*. 2001;21(18):7099–7109.

46. Krajewski S, Krajewska M, Ellerby LM, et al. Release of caspase-9 from mitochondria during neuronal apoptosis and cerebral ischemia. *Proc Natl Acad Sci U S A*. 1999;96(10):5752–5757.

47. Kroemer G, Galluzzi L, Brenner C. Mitochondrial membrane permeabilization in cell death. *Physiol Rev*. 2007;87(1):99–163.

48. Arya A, Meena R, Sethy NK, Das M, Sharma M, Bhargava K. NAP (davunetide) protects primary hippocampus culture by modulating expression profile of antioxidant genes during limiting oxygen conditions. *Free Radic Res*. 2015;49(4):440–452.

49. Aimone JB, Wiles J, Gage FH. Potential role for adult neurogenesis in the encoding of time in new memories. *Nat Neurosci*. 2006;9(6): 723–727.

50. Zhao C, Deng W, Gage FH. Mechanisms and functional implications of adult neurogenesis. *Cell*. 2008;132(4):645–660.

51. Zhu DY, Lau L, Liu SH, Wei JS, Lu YM. Activation of cAMP-response-element-binding protein (CREB) after focal cerebral ischemia stimulates neurogenesis in the adult dentate gyrus. *Proc Natl Acad Sci U S A*. 2004; 101(25):9453–9457.

52. Mair W, Morantte I, Rodrigues AP, et al. Lifespan extension induced by AMPK and calcineurin is mediated by CRTC-1 and CREB. *Nature*. 2011;470(7334):404–408.

53. Steinberg GR, Kemp BE. AMPK in health and disease. *Physiol Rev*. 2009;89(3):1025–1078.

54. Ramamurthy S, Chang E, Cao Y, Zhu J, Ronnett GV. AMPK activation regulates neuronal structure in developing hippocampal neurons. *Neuroscience*. 2014;259:13–24.

55. He L, Sabet A, Djedjos S, et al. Metformin and insulin suppress hepatic gluconeogenesis through phosphorylation of CREB binding protein. *Cell*. 2009;137(4):635–646.

56. Lee TL, Raitano JM, Rennert OM, Chan SW, Chan WY. Accessing the genomic effects of naked nanoceria in murine neuronal cells. *Nanomedicine*. 2012;8(5):599–608.

57. Cimini A, D'Angelo B, Das S, et al. Antibody-conjugated PEGylated cerium oxide nanoparticles for specific targeting of Aβ aggregates modulate neuronal survival pathways. *Acta Biomater*. 2012;8(6):2056–2067.